

# Nuclear spin relaxation in integral and fractional quantum Hall systems

Izabela Szlufarska and Arkadiusz Wójs

*Department of Physics, University of Tennessee, Knoxville, Tennessee 37996,  
and Institute of Physics, Wrocław University of Technology, Wrocław 50-370, Poland*

John J. Quinn

*Department of Physics, University of Tennessee, Knoxville, Tennessee 37996*

(Received 14 February 2002; revised manuscript received 16 July 2002; published 29 October 2002)

We report on a numerical study of the relaxation rates of nuclear spins coupled through the hyperfine interaction to a two dimensional electron gas (2DEG) at magnetic fields corresponding to both fractional and integral Landau level (LL) fillings  $\nu$ . The Hamiltonians of up to 20 interacting electrons are diagonalized exactly in the spherical geometry, neglecting finite layer width, disorder, and LL mixing. The spectral functions  $\tau^{-1}(E)$  describing response of the 2DEG to the reversal of an embedded localized spin are calculated. In a (locally) incompressible  $\nu=1$  or  $\frac{1}{3}$  state, the finite Coulomb energy of short spin waves, together with the small nuclear Zeeman energy, prevent nuclear spin relaxation even in the limit of vanishing electron Zeeman energy ( $E_Z$ ). However, we find that the nuclear spins can couple to the internal excitations of mobile finite-size skyrmions that appear in the 2DEG at sufficiently low  $E_Z$  and at  $\nu$  slightly different from 1 or  $\frac{1}{3}$ . The experimentally observed dependence of nuclear spin relaxation rate on  $E_Z$  and  $\nu$  is qualitatively explained in terms of the occurrence of skyrmions and antiskyrmions of various topological charge.

DOI: 10.1103/PhysRevB.66.165318

PACS number(s): 73.21.Fg, 73.43.-f, 76.60.Es

## I. INTRODUCTION

Two decades ago, transport experiments on two-dimensional electron gas (2DEG) systems in a high magnetic field  $B$  revealed rich physics associated with the unique properties of their charge excitations, including the pair of most striking phenomena, the integral<sup>1,2</sup> and fractional<sup>3-7</sup> quantum Hall effects (IQHE and FQHE). Both effects are the manifestation of a finite gap opening in the charge excitation spectrum at a series of (integral or fractional) values of the Landau level (LL) filling factor  $\nu=1, 2, \frac{1}{3}, \frac{2}{3}, \text{etc.}$ , and of the quasiparticle nature of the elementary charge excitations of this series of gapped (and thus incompressible) ground states.<sup>8,9</sup>

The recent development of nuclear magnetic resonance<sup>10</sup> (NMR) techniques allowed their successful application to the quantum Hall systems,<sup>11-13</sup> and ultimately opened an area of research associated with their spin degree of freedom. Quantum Hall systems with spin excitations are very attractive to both theory and experiment because of their fundamental aspects as well as for potential for applications. They are liquids with unique (Laughlin) correlations<sup>4,14,15</sup> and unique excitations (integrally or fractionally charged quasiparticles without<sup>4</sup> or with<sup>16</sup> spin, skyrmions<sup>17-20</sup> and their collective excitations,<sup>21</sup> and charge<sup>22</sup> and spin waves<sup>23</sup>). On the other hand, the hyperfine coupling of the mobile electron spin excitations to the localized nuclear spins of the underlying atoms<sup>24-26</sup> creates the possibility of controlling the latter by inducing appropriate phase transitions in the 2DEG under a variation of such experimentally adjusted macroscopic parameters as magnetic or electric fields, pressure, or temperature.<sup>27</sup> If using nuclear spin states as a physical realization of quantum bits for storage of (and performing logical operations on) quantum information turned out to be possible, the coupled 2DEG-nuclei system should become a

promising candidate for the spin memory elements of a quantum computer.<sup>28</sup>

The most enlightening experiments on spin quantum Hall systems were those that offered NMR evidence for the occurrence of skyrmions in the IQH (Ref. 12) and FQH (Ref. 13) regimes (confirmed by subsequent optical<sup>29</sup> and transport<sup>27,30</sup> studies). Skyrmions ( $S_K^-$ ) and their conjugates, antiskyrmions ( $S_K^+$ ), consist of  $K$  neutral spin waves bound to a particle in the empty reversed-spin ( $\uparrow$ ) LL or to a hole in the filled ( $\downarrow$ ) LL, respectively.<sup>20</sup> In the IQH regime, the relevant particles are the reversed-spin electrons ( $e_R$ ) and the LL holes ( $h$ ), and the skyrmions can be viewed as  $S_K^- = e_R(e_R h)_K$  or  $S_K^+ = h(e_R h)_K$  bound states, analogous to interband charged excitons  $X_K^\pm$ .<sup>31</sup> In the FQH regime, skyrmions consist of reversed-spin quasielectrons<sup>16</sup> ( $QE_R$ ) and Laughlin quasiholes<sup>4</sup> (QH) bound to form  $S_K^- = QE_R(QE_R QH)_K$  and  $S_K^+ = QH(QE_R QH)_K$ .<sup>20</sup> The analogy between FQH and IQH skyrmions is most evident in the composite fermion (CF) picture,<sup>7</sup> in which  $QE_R$  and QH are represented by particles and holes at the integral filling of their effective CF LL's. In both regimes, skyrmions are charged quasiparticles carrying large spin  $K$ . If the Zeeman energy  $E_Z$  in a sample is sufficiently small for the isolated  $e_R$ ,  $h$ ,  $QE_R$ , and QH quasiparticles to become unstable towards the creation and binding of a number ( $K$ ) of spin waves to form skyrmions, the number of spin flips per particle added to or removed from a filled (electron or CF) LL is  $K$ . This quantity ( $K$ ) sets the slope of the electron spin polarization  $\langle S_z \rangle$ , proportional to the Knight shift measured in the NMR experiments,<sup>12,13</sup> as a function of the filling factor near  $\nu=1, \frac{1}{3}, \text{etc.}$

Of the most recent ones, particularly intriguing seems the NMR experiment of Kuzma *et al.*,<sup>13</sup> which revealed extremely long nuclear spin relaxation time in the FQH regime,

$\tau \leq 0.5$  s, exceeding times recorded earlier<sup>29</sup> by  $\sim 10^3$ . So different a relaxation time found in seemingly similar systems suggest that different microscopic mechanisms can be responsible for nuclear spin relaxation, depending on experimentally variable conditions. Discussion of such mechanisms is the subject of this work.

We report on detailed numerical studies of the hyperfine interaction of the incompressible quantum Hall states at  $\nu = 1$  and  $\frac{1}{3}$ , as well as their spin excitations (spin waves, reversed-spin quasiparticles, and skyrmions), with the localized nuclear spins. The many-electron wave functions are obtained from exact-diagonalization calculations carried out in the Haldane spherical geometry, neglecting disorder and excitations to higher orbital LL's or to higher quantum well subbands. The spectral function  $\tau^{-1}(E)$  that describes the response of the 2DEG to the reversal of an embedded localized spin and governs nuclear spin relaxation time  $\tau$  for the particular microscopic 2DEG-nucleus spin-flip process is calculated.

We find that in a incompressible  $\nu = 1$  or  $\frac{1}{3}$  state, the reversal of a nuclear spin creates a spin wave of a finite wave vector  $k$  simply related to the area occupied by one electron,  $(k\lambda)^2 \approx \nu$  (where  $\lambda$  is the magnetic length). Since the spin wave dispersion  $E_{\text{SW}}(k)$  begins at the electronic Zeeman gap,  $E_{\text{SW}}(0) = E_Z$ , the energy of a spin wave coupled to a nuclear spin exceeds  $E_Z$  by a term  $E_{\text{SW}}(k) - E_{\text{SW}}(0)$ , which is of the order of the characteristic Coulomb energy  $E_C = e^2/\lambda \propto \sqrt{B}$ . Since  $E_Z$  and  $E_C$  are both much larger than the nuclear Zeeman gap, the energy conservation is expected to exclude creation (or annihilation) of spin waves as an efficient mechanism for nuclear spin relaxation. Consequently, very long relaxation times  $\tau$  are expected for nuclear spins embedded in a (locally) incompressible IQH or FQH state, even if  $E_Z$  could be made arbitrarily small (by means of an appropriate doping or an application of pressure).

At  $\nu$  slightly different from 1 or  $\frac{1}{3}$ , skyrmions (or reversed-spin quasiparticles) appear in the incompressible quantum Hall liquid. The response function  $\tau^{-1}(E)$  is calculated for these objects and shown to have peaks corresponding to their "internal spin excitations" in which the skyrmion spin  $K$  and angular momentum  $L$  both change by one ( $S_K \rightarrow S_{K \pm 1}$ ).<sup>19,20</sup> It is also found that the oscillator strength  $\tau_K^{-1}$  of these transitions increases with increasing  $K$ . Since the energy gap for the internal skyrmion excitations is much smaller than  $E_Z$  (and, in particular, it is equal to the nuclear Zeeman gap at the series of values of  $E_Z$ ), the skyrmion-nucleus spin-flip processes will be allowed by the energy conservation law, and provide efficient nuclear spin relaxation mechanism under experimental conditions.

In both IQH and FQH regimes, our results imply critical dependence of the nuclear spin relaxation rate on the presence of skyrmions in the 2DEG (dependent on  $\nu$ ,  $E_Z$ , well width, etc.), in agreement with experiments. However, it is quite remarkable that (because skyrmions of the  $\nu = \frac{1}{3}$  state occur only at much smaller values of  $E_Z$  than skyrmions at  $\nu = 1$ ) the energy required to create an electron spin excitation is much smaller in the IQH regime than in the FQH regime over a long range of  $E_Z$ . This is opposite to the

relation between charge excitation gaps, which scale as  $\hbar\omega_c \propto B$  for IQH states and a (much smaller)  $E_C \propto \sqrt{B}$  for FQH states.

At this stage of our study, we have limited ourselves to the calculation and analysis of a simple spectral function for the idealized many-electron states. This only allows for estimates of *relative* relaxation times  $\tau^{-1}$  for different microscopic processes, but not for their actual magnitudes. The model also neglects the effects of (i) the finite width of the quasi-2DEG, the tilt of the magnetic field, the particular density profile  $\varrho(z)$  in the direction normal to the 2DEG plane, or the nuclear polarization profile  $\varrho_N(z)$  in that direction<sup>26</sup>; (ii) the interaction-induced electron or hole scattering to higher LL's (i.e., LL mixing); (iii) disorder; or (iv) nonequilibrium processes. All these effects may become important in realistic experimental systems, leading to the reduction of the electronic interaction energy scale compared to the nuclear Zeeman energy due to the finite width of electronic wave functions (i) or screening (ii), dependence of the nuclear spin relaxation rate on the correlation between  $\varrho(z)$  and  $\varrho_N(z)$  profiles (i), or localization of electronic excitations that relaxes the angular momentum conservation law in the spin-wave-nucleus or skyrmion-nucleus scattering processes (iii). We plan to study these and other possible effects in the future, and the motivation for the analysis of the ideal model used here is based on the fact that such model allows identification and classification of possible elementary microscopic spin-flip processes, as well as the formulation of the involved selection rules which will be only modified to a various degree depending on the specific experimental conditions.

## II. MODEL

### A. Electron liquid

As an extension of the earlier work on the spin excitations of the 2DEG in the quantum Hall regime,<sup>18,20</sup> we study coupling of these excitations to the localized (e.g., nuclear) spins. The model to describe the 2DEG is that of Ref. 20, except that it is now extended to include the presence of a nucleus. In order to preserve the 2D symmetry of an infinite quantum well in a finite size calculation, the electrons are confined to a Haldane sphere<sup>5</sup> of radius  $R$ . The magnetic field  $B$  normal to the surface is due to a Dirac monopole in the center of the sphere. The monopole strength  $2Q$  is defined in the units of flux quantum  $\phi_0 = hc/e$ , so that  $4\pi R^2 B = 2Q\phi_0$  and  $\lambda = R/\sqrt{Q}$  is the magnetic length. The single-electron states (monopole harmonics) are the eigenstates<sup>5,32</sup> of magnitude ( $l$ ) and projection ( $m$ ) of angular momentum and of spin projection  $\sigma$ , and they form  $g$ -fold ( $g = 2l + 1$ ) degenerate LL's labeled by  $n = l - Q$ .

The cyclotron energy  $\hbar\omega_c \propto B$  is assumed much larger than the Coulomb energy  $E_C = e^2/\lambda \propto \sqrt{B}$ . However, no assumption is made about the electron Zeeman energy, and  $\eta = E_Z/E_C$  is a (small) free parameter of the model. As a result, only the  $\sigma = -\frac{1}{2}$  ( $\downarrow$ ) and  $+\frac{1}{2}$  ( $\uparrow$ ) states of the lowest ( $n = 0$ ) LL need be included in the calculation, denoted simply by  $|m\sigma\rangle$ .

The many-electron Hamiltonian in the lowest LL is

$$H = \sum c_{m_1\sigma}^\dagger c_{m_2\sigma'}^\dagger c_{m_3\sigma'} c_{m_4\sigma} \langle m_1 m_2 | V | m_3 m_4 \rangle + \sum c_{m\uparrow}^\dagger c_{m\uparrow} E_Z, \quad (1)$$

where  $c_{m\sigma}^\dagger$  and  $c_{m\sigma}$  are the electron creation and annihilation operators, the summation goes over all orbital and spin indices, and  $V$  is the Coulomb interaction potential. The  $N$ -electron eigenstates are expanded in the basis of Slater determinants

$$|m_1\sigma_1 \dots m_N\sigma_N\rangle = c_{m_1\sigma_1}^\dagger \dots c_{m_N\sigma_N}^\dagger |\text{vac}\rangle, \quad (2)$$

where  $|\text{vac}\rangle$  is the vacuum state. Basis (2) allows automatic resolution of two good many-body quantum numbers, projections of spin ( $S_z = \sum \sigma_i$ ) and of angular momentum ( $L_z = \sum m_i$ ). However, the lengths of spin ( $S$ ) and of angular momentum ( $L$ ) are resolved numerically in the numerical diagonalization of each ( $S_z, L_z$ ) Hilbert subspace. The additional quantum number  $K = \frac{1}{2}N - S$  measures the number of reversed spins relative to the maximally polarized state. The many-electron states on a (finite) sphere converge to the states on an (infinite) plane in the  $Q = (R/\lambda)^2 \rightarrow \infty$  limit; only the spherical orbital numbers  $L$  and  $L_z$  must be appropriately<sup>33</sup> replaced by the planar ones, the projections of total and center-of-mass angular momentum:  $M$  and  $M_{\text{CM}}$ .

In the lowest energy states of the system described by Hamiltonian (1) near the integral or odd-denominator fractional filling of the lowest LL ( $\nu = 1$  or  $\frac{1}{3}$ ), a small number of spin waves or skyrmions move (to a good approximation, independently) in the appropriate incompressible quantum Hall “background” state. Being charge neutral excitations, spin waves move along straight lines and carry a linear momentum  $\hbar k$ . On a sphere, their linear orbits are closed into great circles, and the linear wave vector  $k$  takes on discrete values following from the quantization of angular momentum,  $L = kR = 0, 1, 2, \dots$ . Skyrmions ( $S_K$ ), on the other hand are charged, particlelike excitations that move along circular cyclotron orbits similar to those of electrons. Their motion is therefore similarly quantized in both geometries, with the lowest LL of states having  $M = M_{\text{CM}} + K$  and  $M_{\text{CM}} = 0, \pm 1, \pm 2, \dots$  (on a plane) or  $L = Q - K$  and  $L_z = L, L - 1, L - 2, \dots$  (on a sphere), respectively.

Both spin waves and skyrmions may become localized in the presence of disorder which has been ignored in this work. However, the dominant effects of such localization, at least in the weak disorder regime, can easily be predicted by analogy with the interband emission of neutral and charged excitons. For spin waves, the localization alters the relative occupation of different  $k$  states (in particular, it increases occupation of the  $k = 0$  state). However, we show later that spin waves do not couple efficiently to nuclear spins regardless of  $k$ . For skyrmions, the localization of their cyclotron orbits in the lower energy areas (without significant distortion of their wave functions) has two consequences: (i) A freezing of the positions of (few) skyrmions relative to

(many) nuclei and thus variation of the electron spin polarization from one nucleus to another; this causes broadening of the Knight shift over the measured sample in the NMR experiment; delocalization of skyrmions and restoration of uniform electron spin polarization at higher temperatures is called the “motional narrowing” of NMR lines. (ii) A variation of skyrmion energies due to confinement relaxes the energy conservation law for the skyrmion-nucleus spin-flip processes, and causes broadenings of the minima of the nuclear spin relaxation time  $\tau$  as a function of  $E_Z$ . Nevertheless, our main conclusions regarding the form of the continuous (due to spin waves) and discrete (due to skyrmions) parts of the 2DEG response function, and the role of the two types of spin excitations for nuclear spin relaxation remain valid independently of localization.<sup>34</sup>

### B. Coupling to nuclear spin

The coupling of the electron system (the “background” quantum Hall state and its spin excitations) to a single isolated localized nuclear spin will be described by the contact hyperfine interaction Hamiltonian<sup>10</sup>

$$F = A \sum_{j,k} \mathbf{I}_k \mathbf{S}_j \delta(\mathbf{r}_j - \mathbf{R}_k), \quad (3)$$

where  $A$  is the coupling constant, and  $\mathbf{S}_j$  and  $\mathbf{I}_k$  ( $\mathbf{r}_j$  and  $\mathbf{R}_k$ ) denote the spin (position) of the  $j$ th electron and  $k$ th nucleus, respectively. Moreover, the distance between nearest nuclei will be assumed sufficiently large to justify neglecting their direct dipolar interaction, and exclude any multi-nucleus phenomena.

Due to the translational/rotational invariance of the 2DEG, the position of the nucleus can be conveniently chosen at the north pole of the sphere, where all electron wave functions of the lowest LL vanish, except for  $|l\uparrow\rangle$  and  $|l\downarrow\rangle$ . Then, ignoring the overall coupling constant (independent of the system size,  $R$  or  $Q$ ), the transverse part of  $F$  describing the spin-flip processes with  $\Delta S_z = 1$  and projected onto the lowest LL simplifies to

$$F = c_{l\uparrow}^\dagger c_{l\downarrow}. \quad (4)$$

Clearly, the reversal of the localized (nuclear) spin is accompanied by a reversal of an electronic spin spread over a (cyclotron) orbit of finite radius  $\sim \lambda$ .

According to the Fermi golden rule, the oscillator strength  $\tau_{if}^{-1}$  for the transition between a given pair of initial and final electronic eigenstates,  $|i\rangle$  and  $|f\rangle$ , is proportional to the square of the matrix element of  $F$ ,

$$\tau_{if}^{-1} = |\langle f | F | i \rangle|^2, \quad (5)$$

and, accordingly, the spectral function for a given initial (ground) state is

$$\tau^{-1}(E) \equiv \tau_i^{-1}(E) = \sum_f \tau_{if}^{-1} \delta[E - (E_i - E_f)], \quad (6)$$

where  $E_i$  and  $E_f$  are the energies of the initial and final states, respectively. Also, from Eq. (4),  $F$  couples the electron states with equal  $L_z$  and  $S_z$  different by one.

Note that  $\tau^{-1}(E)$  is only defined up to a coupling constant that we are unable to calculate. Therefore, when comparing our results with experiment, only the relative intensities of different microscopic spin-flip processes (e.g., processes that involve spin waves with different  $k$ , skyrmions with different  $K$ , or skyrmions as opposed to spin waves) are meaningful, but we are unable to estimate the actual magnitude of the nuclear spin relaxation rates. However, only these relative intensities are a universal property of the electron quantum Hall system, virtually independent of many experimentally variable parameters (electron density, nuclear spin polarization profile across the 2DEG plane,<sup>26</sup> etc.). While spectral function (6) captures the essential physics of the interaction between an (ideal) Laughlin liquid and localized spins, the details of both the liquid and the spins must be included in a realistic calculation of the relaxation rates.

Due to the simple form of the operator  $F$  in our basis [Eq. (2)], the oscillator strengths can be easily evaluated for any known pair of  $|i\rangle$  and  $|f\rangle$  eigenstates. Therefore, the most difficult computational task is the accurate calculation of the many-electron eigenfunctions. Moreover, because of the breaking of both spatial and spin symmetry by the operator  $F$ , entire multiplets with different  $L_z$  and  $S_z$  must be calculated for each  $L$  and  $S$ . Hence the proper identification of the relevant many-electron eigenstates that (i) describe a planar system in the  $R/\lambda \rightarrow \infty$  limit, and (ii) have significant  $\tau^{-1}$ , becomes essential.

### III. INTEGRAL QUANTUM HALL REGIME

#### A. Spin waves

We begin with the integral quantum Hall regime and the filling factor of precisely  $\nu=1$ . We numerically evaluate the oscillator strengths  $\tau^{-1}$  for all possible transitions induced by the operator  $F$  from the initial nondegenerate incompressible IQH ground state with  $L=0$ ,  $S_z = -\frac{1}{2}N$ , and  $K=0$ . From the commutator  $[F, S^2]$  it can easily be shown that the spin-flip transition defined by  $F$  couples the  $K=0$  initial state  $|i\rangle$  to two different subspaces, with  $K=0$  or 1. However, the length of the total projection of  $F|i\rangle$ , the vector obtained by acting by  $F$  on the initial IQH ground state, onto the  $K=0$  subspace equals  $N^{-1}$  in a finite  $N$ -electron initial state, and thus it disappears in the  $N \rightarrow \infty$  limit. Therefore, not surprisingly, the only spin excitations coupled to an infinite (planar)  $\nu=1$  state by  $F$  are those with  $K=1$ . Of these, the only ones with significant oscillator strength  $\tau^{-1}$  turn out to be the spin wave states, which at the same time are the lowest energy excitations at  $\nu=1$ .

The numerical results for the spin-flip transitions corresponding to creation (annihilation) of spin waves in a finite  $\nu=1$  state of  $N=20$  electrons at  $2Q=N-1=19$  are shown in Fig. 1(a). In this and all other spectra in the paper  $E$  stands for the energy difference between the final and initial states and is given in the units of  $E_C = e^2/\lambda$ . The Zeeman energy  $E_Z$  is not included. The horizontal axis shows the total angu-

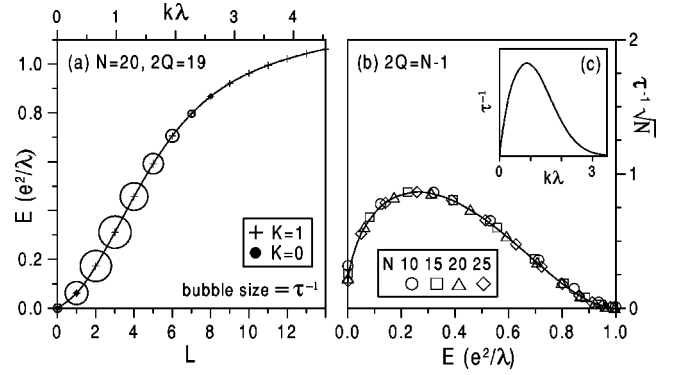


FIG. 1. (a) The spin wave energy spectrum (energy  $E$  vs angular momentum  $L$  and wave vector  $k$ ) at  $\nu=1$  calculated for  $N=20$  electrons on Haldane sphere. The bubble diameters give the oscillator strength  $\tau^{-1}$  for the spin wave emission coupled to the nuclear spin reversal. (b) The response function of a planar  $\nu=1$  state to a nuclear spin reversal (oscillator strength  $\tau^{-1}$  calculated on a sphere for different  $N \leq 25$  and normalized by  $\sqrt{N}$  vs energy  $E$ ). (c) The response function  $\tau^{-1}$  shown as a function of wave vector  $k$ . The Zeeman energy  $E_Z$  is excluded, and  $\lambda$  is the magnetic length.

lar momentum  $L$  (for the spin waves,  $L=kR$ ), and the oscillator strength  $\tau^{-1}$  is proportional to the diameter of a bubble around each energy level marked with a cross.

As could be predicted from Eq. (4), the reversal of an electronic spin induced by  $F$  occurs over an area corresponding to a cyclotron orbit. This sets a characteristic length scale  $\xi \sim \lambda$  for the efficient spin-flip process, and indeed in Fig. 1(a)  $\tau^{-1}$  has a maximum at a finite  $L$ , while it vanishes in the limits of both small and large  $L$ .

To determine the spectral function of a  $\nu=1$  state of an infinite 2DEG we have compared data obtained for different electron numbers,  $N \leq 25$ , and plotted the results together in Fig. 1(b). The oscillator strengths for discrete values of  $E$  are multiplied by the factor  $\sqrt{N} \propto \sqrt{Q} \propto R/\lambda$ , which comes from normalization of the wave function of the extended spin wave over the entire sphere. All data points lie nicely on one regular curve that describes the spin wave creation/annihilation in both finite (spherical) and infinite (planar) systems. As it is the characteristic wave vector  $k$  (through the characteristic length scale  $\xi$ ) rather than the energy  $E$  that determines the position of the maximum of  $\tau^{-1}$ , in the inset (c) we replot it as a function of  $k$  [only setting  $\tau^{-1}(0)$  to zero as appropriate for an infinite system].  $\tau^{-1}(k)$  is a more universal characteristic of the  $\nu=1$  IQH state than  $\tau^{-1}(E)$  in a sense that the spin wave dispersion  $E_{SW}(k)$ , in an ideal 2D system derived by Kallin and Halperin,<sup>23</sup> in experiment it may also depend on additional characteristics of actual 2DEG (e.g., the well width). As expected,  $\tau^{-1}(k)$  has a maximum at  $k \sim \lambda^{-1}$ , which defines the spin-flip length scale of  $\xi \sim \lambda \propto \sqrt{B}$ .

Based on Fig. 1, we make the following observations: (i) The incompressible  $\nu=1$  liquid responds to the reversal of a localized spin by emission of a spin wave whose kinetic energy,  $E_{SW}(k)$ , increases as a function of  $k$ . (ii) The response function  $\tau^{-1}(E)$  vanishes in both  $k=0$  and  $\infty$  limits, and it reaches maximum at  $E$  corresponding to  $k \sim \lambda^{-1}$ . (iii)

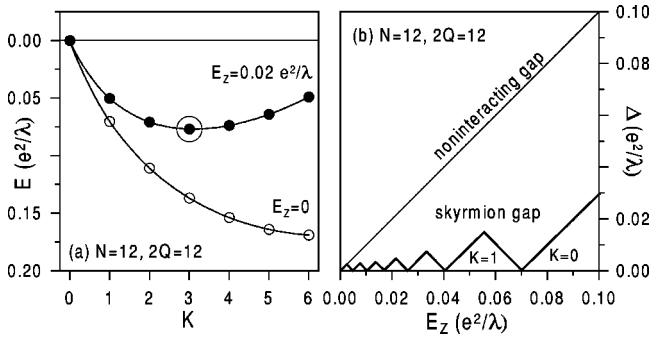


FIG. 2. (a) The skyrmion energy spectrum (energy  $E$  vs reversed spin number  $K$ ) at  $\nu=1^\pm$  calculated for  $N=12$  electrons on Haldane sphere. Open and full symbols correspond to the Zeeman energy  $E_Z=0$  and  $0.02 e^2/\lambda$ , respectively ( $\lambda$  is the magnetic length). (b) The energy gap  $\Delta$  for skyrmion spin excitations ( $S_K \rightarrow S_{K\pm 1}$ ) at  $\nu=1^\pm$  as a function of  $E_Z$ , compared to the spin wave gap  $\Delta = E_Z$  at  $\nu=1$ .

When electron Zeeman energy is added, the energy of a  $k \sim \lambda^{-1}$  spin wave that can couple to a localized spin reversal is a sum of two terms,  $E_Z$  and  $E_{SW}(\lambda^{-1})$ . (iv) Since  $E_{SW}(\lambda^{-1}) \approx \frac{1}{4} E_C$  (in an ideal system<sup>23</sup>) is typically much larger than the nuclear Zeeman energy, the energy conservation prevents efficient relaxation through emission of spin waves in a (locally) incompressible liquid regardless of the value of  $E_Z$ .

This weak coupling of the  $\nu=1$  state to the nuclear spins obtained above agrees well with long nuclear spin relaxation times measured at this filling factor at low temperatures.<sup>12</sup> It is evident from the experiments showing rapid increase of the relaxation rate when either  $\nu$  is moved away from 1 or temperature is elevated (from 2.1–4.2 K) (Ref. 12) that charged excitations provide more efficient mechanism for nuclear spin relaxation than the spin waves. Let us then move on to an analysis of the spin-flip processes in the presence of such excitations, reversed-spin quasiparticles and skyrmions.

### B. Skyrmions

It is well-known that an extra particle (a reversed-spin electron or a spin hole) added to the  $\nu=1$  ferromagnetic ground state induces and binds spin waves (whose number  $K$  depends on  $E_Z/E_C$ ) to form a skyrmion<sup>18</sup> ( $S_K$ ), a particlelike charged excitation carrying a (possibly large) spin  $K$ . In Fig. 2(a) we replot the (anti)skyrmion energy spectrum calculated earlier in Ref. 20 for  $N=12$  electrons at  $2Q=12$ . Using the exact particle-hole symmetry within an isolated LL, this state can be mapped onto one in which an extra reversed-spin electron is added to the  $\nu=1$  state at the same value of  $2Q=12$ , and hence it will be denoted here as  $\nu=1^\pm$ . Again, the vertical axis gives the skyrmion energy  $E$  measured from the maximally polarized ( $K=0$ ) state which in this case corresponds to one spin hole in the  $\nu=1$  state. On the horizontal axis we show the skyrmion spin (or size),  $K$ , which is also related<sup>20</sup> to its angular momentum,  $L=Q-K$ .

The open symbols in Fig. 2(a) mark the skyrmion energy spectrum  $E_S(K)$ , excluding the Zeeman energy. In an infinite

system (and not only at  $\nu=1$ , but also in the FQH regime discussed in the following section), it can be quite accurately approximated by  $E_S(K) \approx -\mathcal{E} [K/(K+1)]^\alpha$ . In an ideal 2D system, the binding energy of an infinite skyrmion at  $\nu=1$  is known exactly,<sup>18</sup>  $\mathcal{E} = \frac{1}{4} \sqrt{\pi/2} E_C$ , and any choice of  $\alpha \sim 1$  captures the most essential feature of  $E_S(K)$ , which is that  $E_S(K-1) - E_S(K) > E_S(K) - E_S(K+1)$  for each  $K$ .

Although our numerics yields  $\alpha \approx 1.7$  at  $\nu=1$ , it is quite illuminating to solve the simplest case of  $\alpha=1$  (the equally simple arithmetics for  $\alpha=2$  gives essentially identical answer; moreover, for  $\nu=\frac{1}{3}$  it actually seems that  $\alpha \approx 1$ ). When the Zeeman term  $KE_Z$  is added to the skyrmion energy as shown with full dots in Fig. 2(a) the ground state becomes a finite-size skyrmion with a certain  $K$  (as marked with an open circle, for  $E_Z=0.02 E_C$  it turns out to be  $K=3$ ). Using our simple model

$$E_S(K) = -\mathcal{E} \frac{K}{K+1} + KE_Z, \quad (7)$$

we obtain that the transition between the  $S_{K-1}$  and  $S_K$  ground states occurs at  $E_Z = \mathcal{E}/[K(K+1)]$  (in particular, the smallest skyrmion,  $S_1$ , is stable below  $E_Z = \frac{1}{2}\mathcal{E}$ ), and the excitation gap  $\Delta_K$  from  $S_K$  to the lower of the  $S_{K-1}$  or  $S_{K+1}$  states [it is plotted in Fig. 2(b) for the numerical data of Fig. 2(a)] reaches its maximum value of  $\Delta_K = \mathcal{E}/[K(K+1)(K+2)]$  at  $E_Z = \mathcal{E}/[K(K+2)]$ .

As seen in Fig. 2(b), the most striking feature of the skyrmion energy spectrum in the presence of the (sufficiently small) Zeeman energy is that, in contrast to the spin wave spectrum of the (locally) incompressible IQH liquid, the gap for spin excitations is greatly reduced compared to (and largely independent of)  $E_Z$ . Indeed, it follows from our expression for the maximum of  $\Delta_K$  that  $\Delta_K/E_Z \leq (K+1)^{-1}$  and  $\Delta_K/E_Z \leq \sqrt{E_Z/\mathcal{E}}$ . Moreover, the gap skyrmion  $\Delta_K$  can be brought to resonance with an arbitrarily small nuclear Zeeman energy at the at entire series of  $E_Z$  near the  $S_{K-1} \leftrightarrow S_K$  transitions.

Being charged objects, skyrmions move along electron-like cyclotron orbits and repel one another through an effective short-range pseudopotential similar to that of electrons in the lowest LL.<sup>20</sup> Such a short-range repulsion causes Laughlin correlations between the skyrmions,<sup>15</sup> which therefore avoid high energy collisions with one another and behave as well-defined quasiparticles moving independently in the underlying IQH liquid. We know that in a similar, electron–valence-hole system, Laughlin correlations of interband charged excitons ( $X^-$ ) with one another as well as with surrounding electrons simplify the photoluminescence of a dilute ( $\nu < \frac{1}{3}$ ) 2DEG to the recombination of spatially isolated  $X^-$ 's.<sup>35</sup> By analogy, we expect that the many-skyrmion effects can be excluded from the skyrmion-nucleus spin-flip scattering.

To verify the possibility of efficient nuclear spin relaxation through the interaction with skyrmions, we have evaluated the spectral functions  $\tau_i(E)$  for the initial state  $|i\rangle$  corresponding to a single skyrmion (or antiskyrmion) in a finite,  $N$ -electron  $\nu=1$  system. Due to the finite size of the skyrmion, its ground state is a degenerate electron-like LL. On a

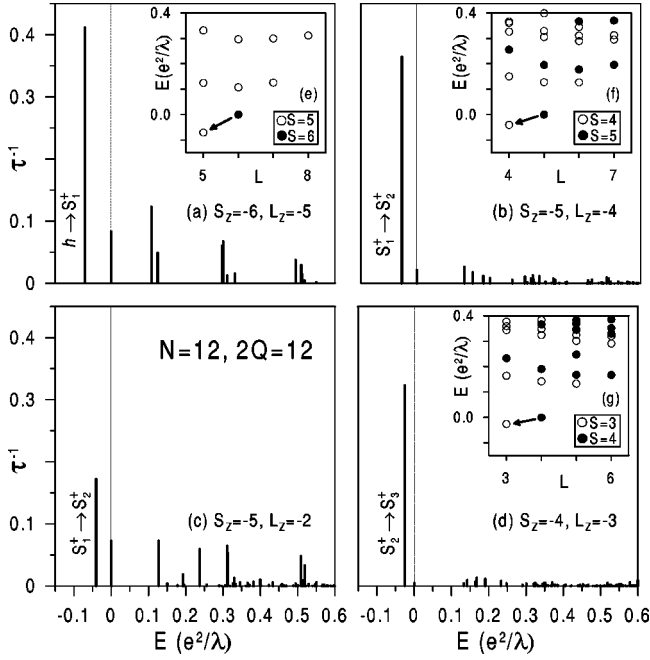


FIG. 3. The spectral function of the hyperfine transition operator  $F$  (oscillator strength  $\tau^{-1}$  vs. energy  $E$ ) at  $\nu=1^\pm$  calculated for  $N=12$  electrons on Haldane sphere. Strong peaks at  $E<0$  correspond to the “internal” skyrmion transitions  $S_K \rightarrow S_{K+1}$  indicated with arrows in the energy spectra shown in insets (e)–(g).  $L_z$  is the skyrmion angular momentum projection related to the impact parameter of the skyrmion–nucleus collision. Different frames correspond to different initial electron states:  $h$  (a),  $S_1^+$  (b), and  $S_2^+$  (d) close to the nucleus, and  $S_1^+$  farther from the nucleus (c). The Zeeman energy  $E_Z$  is excluded and  $\lambda$  is the magnetic length.

Haldane sphere, this LL is represented by the angular momentum multiplet at  $L=Q-K$ . Different values of  $L_z = -L, -L+1, \dots, L$  label different cyclotron orbits, and the closest orbit to the north pole (the position of the nucleus) is that with  $L_z=L$  for a skyrmion ( $S_K^-$ ) and  $L_z=-L$  for an antiskyrmion ( $S_K^+$ ). Clearly, the value of  $\tau_{if}$  for a given  $i \rightarrow f$  transition involving a skyrmion depends on  $L_z$ , which plays the role of an impact parameter of the skyrmion–nucleus collision.

We have numerically studied a few systems with different values of  $N$  and  $2Q=N$ . For each  $N$  we have calculated the complete  $\tau_{if}$  spectra corresponding to the (anti)skyrmionic initial states  $|i\rangle = S_0^+, S_1^+, S_2^+, \dots$  with different values of  $L_z$ , and to all possible finite states  $|f\rangle$ . As an example, in Fig. 3 we show the results for  $N=12$  and the initial states with  $K=0, 1$ , and  $2$  (for  $K=1$  data for two values of  $L_z$  are shown). The transition energy given on the horizontal axis is  $E = E_f - E_i$  (excluding  $E_Z$ ), and the units of  $\tau^{-1}$  on the vertical axis follow from Eq. (4). In the insets we display the corresponding energy spectra in which the initial skyrmion states as well as all the final states can be identified for each transition.

All the spectra are quite similar in that they can be decomposed into the quasicontinuous part at  $E>0$  (here discrete because of size quantization) due to the response of the underlying IQH state discussed in the preceding subsection,

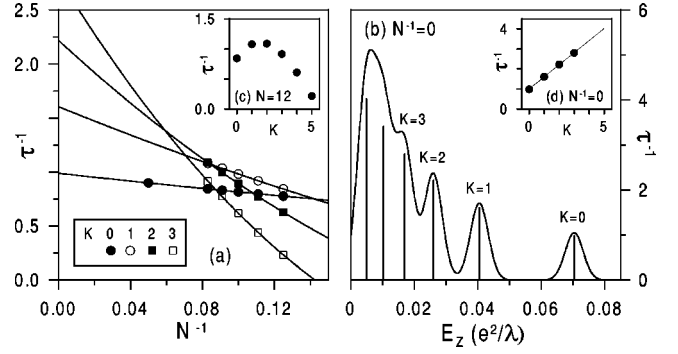


FIG. 4. (a) The oscillator strengths  $\tau^{-1}$  of the “internal” skyrmion transitions  $S_K \rightarrow S_{K+1}$  induced by a nuclear spin reversal, as a function of the inverse electron number,  $N^{-1}$ . (b) Same  $\tau^{-1}$ , but calculated in a finite,  $N=12$  electron system and plotted as a function of the skyrmion spin  $K$ . (c) Same  $\tau^{-1}$ , but extrapolated to  $N \rightarrow \infty$  and plotted as a function of the Zeeman energy  $E_Z$ . The position of each peak is the value of  $E_Z$  at which the transition energy  $\Delta$  is zero. The solid line includes Gaussian broadening. (d) Same as (b), but for data extrapolated to  $N \rightarrow \infty$ .

and a single peak at  $E<0$  due to a  $S_K \rightarrow S_{K+1}$  transition. Since we are mostly interested in the processes that may conserve energy to allow efficient nuclear spin relaxation, let us neglect all  $E>0$  transitions and concentrate on the  $S_K \rightarrow S_{K+1}$  one, whose energy including  $E_Z$  can be made equal to the nuclear Zeeman gap. Clearly, it is only allowed for  $|L_z| \leq Q - (K+1)$  and its intensity quickly decreases when  $L_z$  is increased from the minimum allowed value (such increase of  $L_z$  corresponding to an increase of the nucleus–skyrmion average separation before the collision, i.e., of the impact parameter). Because we assume no localization and thus allow that a skyrmion moves freely over the position of the nucleus (placed at the north pole by an arbitrary choice), it is more physical to consider  $\tau^{-1}$  summed over all allowed values of  $L_z$  as a characteristic of this “internal skyrmion transition.”

In order to complete the analysis of the role of skyrmions in nuclear spin relaxation, to the facts that the skyrmion–nucleus spin scattering has a finite oscillator strength and that it can conserve energy, we ought to add the dependence on the skyrmion size,  $K$ . In Fig. 4(b) we display the total (summed over all  $L_z$ ) values of  $\tau^{-1}$  for the  $S_K \rightarrow S_{K+1}$  transitions calculated for  $N=12$  and plotted as a function of  $K$ . Surprisingly, the function  $\tau^{-1}(K)$  has a maximum at a finite  $K$ . In order to estimate  $\tau^{-1}$  in an infinite system, we have recalculated  $\tau^{-1}(K)$  for different  $N$ . The results are shown in Fig. 4(a) where we plot  $\tau^{-1}$  for  $K=0, 1, 2$ , and  $3$  as a function of the inverse system size,  $N^{-1}$ . The very regular dependence of  $\tau^{-1}$  on  $N^{-1}$  for each  $K$  allows their accurate (quadratic) extrapolation to the  $N^{-1} \rightarrow 0$  limit, as indicated by the solid lines. The result of the extrapolation is that in an infinite (planar) system,  $\tau^{-1}$  increases monotonically with increasing  $K$ , which indicates that the nonmonotonic behavior in Fig. 4(b) is an artifact.

The nearly linear increase of the extrapolated values of  $\tau^{-1}$  with increasing  $K$  shown in Fig. 4(d) suggests that the total intensity  $\tau^{-1}$  (summed over all  $L_z$ ) depends predomi-

nantly on the skyrmion area. Because in experiments the differential cross section for the skyrmion-nucleus collisions also depends on the skyrmion area, one can also expect that the nuclear relaxation rate will increase as a function of  $K$  (at a constant number of skyrmions). In Fig. 4(c) we plot the  $\tau^{-1}$  peaks corresponding to subsequent  $S_K \rightarrow S_{K+1}$  transitions as a function of  $E_Z$  at which the energy of this transition ( $E$ ) vanishes [compare Fig. 2(b) in which the closing of the gap is shown]. Assuming that the skyrmion-nucleus spin scattering is a dominant nuclear spin relaxation process, and that it is most efficient when  $E \approx 0$ , the curves obtained by broadening of the discrete peaks with Gaussians imitate the nuclear spin relaxation rate as a function of  $E_Z$ . It is remarkable that when the value of  $E_Z$  is lowered, the peaks with higher  $K$  are selected from the spectral function, the separation between the neighboring peaks decreases and their intensity increases. Let us stress that this expected behavior for  $\nu = 1^\pm$  differs qualitatively from what we predict at precisely  $\nu = 1$ , where the relaxation rate should increase monotonically with decreasing  $E_Z$  and remain small even at  $E_Z = 0$ .

#### IV. FRACTIONAL QUANTUM HALL REGIME

Recent NMR (Ref. 13) and optical<sup>29</sup> experiments near  $\nu = \frac{1}{3}$  revealed a similar dependence of the electron spin polarization on the magnetic field to that found earlier at  $\nu = 1$ . In contrast to an earlier prediction,<sup>36</sup> it now seems plausible that the fast and weakly temperature-dependent nuclear spin relaxation near  $\nu = \frac{1}{3}$  is somehow related to the presence of skyrmions in the Laughlin liquid.

Near  $\nu = (2p+1)^{-1}$  ( $p \geq 1$  is an integer) Laughlin correlations<sup>4</sup> allow a mapping<sup>7</sup> of the low-energy interacting electron states onto the noninteracting composite fermion (CF) states with an effective filling factor  $\nu^* \approx 1$ . The Chern-Simons transformation, in which  $2p$  magnetic flux quanta are attached to each electron, results in an effective CF LL degeneracy of  $g^* = g - 2p(N-1)$ . On a sphere,<sup>5</sup> this replaces the electronic single particle angular momentum  $l = Q \approx \frac{1}{2}(2p+1)(N-1)$  by an effective CF angular momentum  $l^* = Q^* \approx \frac{1}{2}(N-1)$ , where  $2Q^*$  denotes the effective CF monopole strength.

There are two types of low energy charge-neutral excitations of Laughlin  $\nu = \frac{1}{3}$  ground state, similar to the charge and spin waves<sup>23</sup> of the  $\nu = 1$  state. This similarity lies at the heart of the CF picture,<sup>7</sup> where these excitations correspond to promoting one CF from a completely filled lowest ( $n=0$ ) spin- $\downarrow$  CF LL either to the first excited ( $n=1$ ) CF LL of the same spin ( $\downarrow$ ) or to the same CF LL ( $n=0$ ) but with the reversed spin ( $\uparrow$ ). Similarly to  $\nu = 1$ , charge and spin waves at  $\nu = \frac{1}{3}$  are composed of three types of elementary quasiparticles: a hole in the  $n=0$  spin- $\downarrow$  CF LL and the particles in the  $n=1$  spin- $\downarrow$  and  $n=0$  spin- $\uparrow$  CF LL's, representing the Laughlin quasihole (QH) and quasielectron (QE) and the reversed-spin quasielectron (QE<sub>R</sub>), respectively. Each of these quasiparticles is characterized by such single-particle quantities as (fractional) electric charge, energy, or Landau degeneracy of the single-particle Hilbert space.

Expecting a similar behavior, we have carried out similar

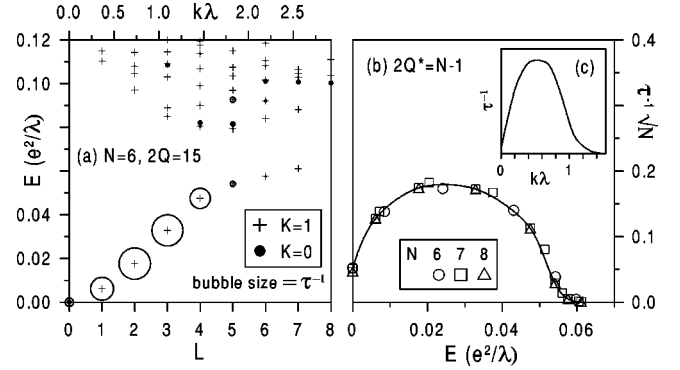


FIG. 5. Same as Fig. 1 but for  $\nu = \frac{1}{3}$ . More excited states appear in frame (a) in addition to the spin wave.

calculations for the  $\nu \approx \frac{1}{3}$  filling as described in Sec. III for  $\nu \approx 1$ . Let us begin with the Laughlin incompressible FQH state at precisely  $\nu = \frac{1}{3}$ . We found that the reversal of a nuclear spin in this state creates a spin wave, in perfect analogy to what happened in the IQH regime. The main difference is that the spin wave at  $\nu = \frac{1}{3}$  consists of a QE<sub>R</sub>-QH pair whose interaction energy scale is about an order of magnitude smaller than it was for a  $e_R$ - $h$  pair at  $\nu = 1$ , predominantly due to the fractional QE<sub>R</sub> and QH charge (but also due to a larger size of the QE<sub>R</sub> and QH wave functions). In Fig. 5 we show the graphs for the FQH regime similar to those of Fig. 1. The spectrum shown in Fig. 5(a) is for  $N = 6$  electrons at  $2Q = 15$ . In the CF picture, this corresponds to six CF's filling exactly their lowest spin- $\downarrow$  LL of degeneracy  $g^* = 2Q^* + 1 = 6$ . Similarly to  $\nu = 1$ , additional weak transitions to higher states appear in a small system, but the spin wave will remain the dominant feature of the spectrum in the  $N \rightarrow \infty$  limit.

In Fig. 5(b) we overlay the spin wave spectra  $\tau^{-1}(E)$  obtained for different values of  $N$ . Similarly to  $\nu = 1$ , all data points (with  $\tau^{-1}$  multiplied by  $\sqrt{N}$ ) fall on the same regular curve which, as expected, vanishes in both  $E = 0$  and  $E = \infty$  limits, and reaches maximum at the energy  $E \approx 0.025 E_C$ , about an order of magnitude smaller than at  $\nu = 1$ . In Fig. 5(c) we replot  $\tau^{-1}$  as a function of wave vector  $k = L/R$ . By analogy to  $\nu = 1$ , we expect that the length of spin wave most strongly coupled by  $F$  to a nuclear spin reversal corresponds to the smallest area containing one electron (and thus containing one unit of electron spin that must flip to compensate for the nuclear spin). For the uniform  $\nu = \frac{1}{3}$  state, the average area per electron is three times larger than at  $\nu = 1$ , yielding  $\sqrt{3}$  times larger length scale  $\xi$ , and thus the maximum of  $\tau^{-1}(k)$  is expected at  $k = \xi^{-1} \sim (\sqrt{3}\lambda)^{-1} \approx 0.58\lambda^{-1}$ . Indeed, this seems to be true of our Fig. 5(c).

To summarize our results at precisely  $\nu = \frac{1}{3}$ , the mechanism of the coupling to the nuclear spins is very analogous. The two major differences can be predicted from the simple arguments of the three times reduced electron density and the three times reduced charge of the involved quasiparticles. These differences are (i) about a  $\sqrt{3}$  times larger characteristic length scale of the response  $\xi$  (wave length of the “active” spin wave) and (ii) about a  $3^2$  smaller interaction energy  $E_{SW}(\xi^{-1})$  of such active spin wave. While (i) is the

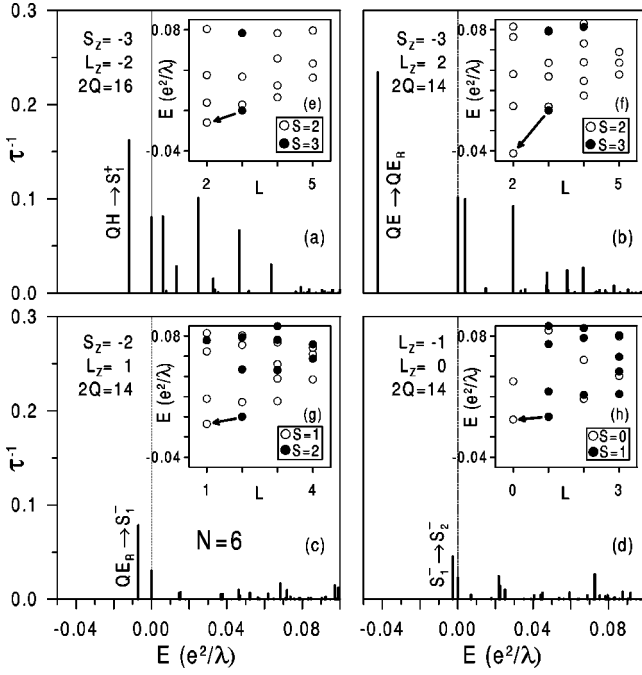


FIG. 6. Same as Fig. 3 but for  $\nu = \frac{1}{3}$ . The initial states in different frames are QH (a), QE (b),  $QE_R$  (c), and  $S_1^-$  (d).

reason for the *reduction* of  $\tau^{-1}$  of the corresponding transitions (compare the maxima of  $\sqrt{N}\tau^{-1}$  in Figs. 1 and 5), (ii) should actually *enhance* nuclear relaxation due to spin waves (if  $E_Z$  can be made disappear) as a result of the weaker violation of the energy conservation.

Let us now turn to the spin-flip processes involving FQH skyrmions. Their energy spectra and gaps for the “internal” excitations are very similar to those at  $\nu=1$  except for an overall reduction of the interaction energy scale and breaking of the skyrmion–antiskyrmion symmetry.<sup>20</sup> In particular, graphs analogous to those in Fig. 2 describe also the FQH skyrmions, only with about an order of magnitude smaller critical values of  $E_Z$ .

In Fig. 6 we display some of the  $\tau^{-1}(E)$  spectra calculated for  $N=6$  electrons at  $2Q^*=N$  and  $N+2$ , corresponding to one skyrmion (or QE, or  $QE_R$ ) and antiskyrmion (or QH) in the Laughlin  $\nu = \frac{1}{3}$  state, respectively. As in Fig. 3, in the insets we show the energy spectra in which the initial and final states for each transition can be found. In perfect analogy to the IQH system, we identify the sequences of  $F$ -induced transitions with  $E < 0$  that occur between the skyrmion or antiskyrmion states of different  $K$ :  $QE \rightarrow QE_R \rightarrow S_1^- \rightarrow S_2^- \rightarrow \dots$  and  $QH \rightarrow S_1^+ \rightarrow S_2^+ \rightarrow \dots$ .

## V. COMPARISON OF IQH AND FQH REGIMES

Let us finally compare the skyrmion and spin wave excitations and their possible coupling to the nuclear spins in the IQH and FQH regimes. It turns out that the following behavior depicted in Fig. 7 that can be predicted from the simple arguments and existing analytical results alone is not far from the results of our exact calculations. The skyrmion energy spectrum is adequately reproduced by Eq. (7), with  $\mathcal{E}$

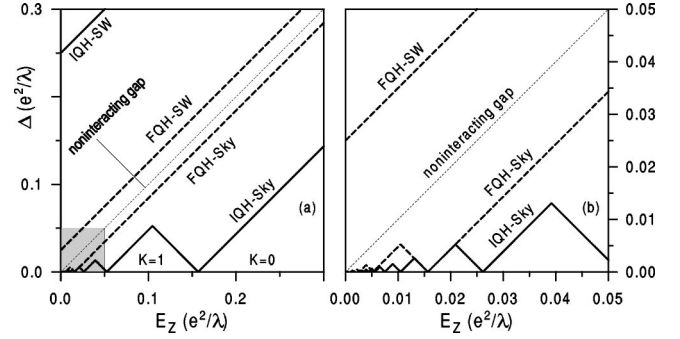


FIG. 7. The comparison of transition energies  $\Delta$  of IQH and FQH systems corresponding to the spin wave emission and the internal skyrmion excitations, obtained from Eq. (7).  $E_Z$  is the Zeeman energy and  $\lambda$  is the magnetic length. Frame (b) shows a blow up of the shaded part of frame (a).

$= \frac{1}{4} \sqrt{\pi/2} E_C$  for the IQH regime,<sup>18</sup> and about a ten times smaller value for the FQH regime. This determines the dependence of the skyrmion size  $K$  and its gap  $\Delta$  for spin excitations ( $S_K \rightarrow S_{K\pm 1}$ ) on  $E_Z$  in both regimes. These plots of  $\Delta(E_Z)$  are marked as “IQH-Sky” and “FQH-Sky” in Fig. 7. On the other hand, it follows from the fact that  $\lambda$  is the size of a cyclotron orbit that the spin waves must have  $k \sim \lambda^{-1}$  to strongly couple to a localized spin reversal at  $\nu = 1$ . Also, knowing<sup>23</sup> the spin wave dispersion  $E_{SW}(k)$  allows one to estimate the total (Zeeman plus Coulomb) energy gap for such “active” IQH spin waves,  $\Delta \sim E_Z + \frac{1}{4} E_C$ . By reducing the interaction energy by an order of magnitude one can also predict the spin wave gap in the FQH regime,  $\Delta \sim E_Z + \frac{1}{40} E_C$ . These two plots of  $\Delta(E_Z)$  are marked as “IQH-SW” and “FQH-SW” in Fig. 7.

Since the energy conservation requires that  $\Delta$  be equal or at least close to the nuclear Zeeman energy which is essentially zero, it is clear from Fig. 7 how the relative efficiencies of spin waves and skyrmions in both regimes depend on  $E_Z$ . It is noteworthy that the ( $e_R$ - $h$  or  $QE_R$ -QH) interactions can have different effect on the spin gap  $\Delta$ , depending on the presence of skyrmions in the system. Compared to a noninteracting system for which  $\Delta = E_Z$ , the interactions *increase* the spin gap  $\Delta$  associated with the creation of spin waves, but *decrease* such a gap associated with the skyrmion excitations. For spin waves, the enhancement of  $\Delta$  is due to a decrease of  $e_R$ - $h$  or  $QE_R$ -QH attraction at a finite wave vector  $k \sim \sqrt{\nu}/\lambda$  (that can be interpreted as a spin wave kinetic energy). For skyrmions, the reduction of  $\Delta$  is due to interaction induced level crossings and ground state transitions.

It is clear from Fig. 7 that the strong interactions in the IQH regime prevent the spin waves at  $\nu=1$  from coming into resonance with nuclear spins regardless of the value of  $E_Z$ , and practically eliminate them as an efficient nuclear spin relaxation mechanism at this filling. But at the same time, these interactions allow efficient relaxation near  $\nu=1$  through the spin-flip nucleus-skyrmion collisions over a long range of  $E_Z$ . On the other hand, the much weaker interactions in the FQH regime do not completely exclude nuclear relaxation by means of spin wave emission at  $E_Z \approx 0$ , but they considerably shorten the range of  $E_Z$  in which the skyr-



mions occur and can spin-flip collide with the nuclei. Therefore, a drop of the nuclear spin relaxation time  $\tau$  caused by the introduction of charge excitations to the incompressible liquid (by varying density or magnetic field to move  $\nu$  away from 1 or  $\frac{1}{3}$ , increasing temperature, or inducing current) should be more pronounced in the IQH regime. This agrees with the experiments that typically show much longer relaxation times at  $\nu=1$  than at  $\nu=\frac{1}{3}$ .

## VI. CONCLUSION

Using exact numerical diagonalization techniques we have studied possible relaxation mechanisms of nuclear spins coupled through the hyperfine interaction to the quantum Hall states of a 2DEG at filling factors near  $\nu=1$  and  $\frac{1}{3}$ . By extrapolation of our finite-size results, we were able to determine the spectral function  $\tau^{-1}(E)$  describing the response of an infinite (planar) 2DEG to the reversal of an embedded localized spin. We found that the spectral function can be decomposed into a continuous part describing transitions from the incompressible “background” state, and a discrete part which is due to the presence of additional charge excitations (skyrmions).

The continuous part of the response function  $\tau^{-1}(E)$  describes the emission of a spin wave, whose energy  $E_{sw}$  is a sum of the electronic Zeeman gap  $E_Z$  and a kinetic energy dependent on the wave vector  $k$ . We found that, when expressed as a function of wave vector,  $\tau^{-1}$  vanishes in both  $k=0$  and  $\infty$  limits, and that it has a maximum at a finite  $k \approx \lambda^{-1}\sqrt{\nu}$ . Using the known spin wave dispersion for  $\nu=1$ , we showed that the emission energy of an “active” spin wave that can couple to a nuclear spin reversal exceeds  $E_Z$

by a kinetic term  $\sim \frac{1}{4}E_C\nu^2$ . This implies that even in the limit of vanishing  $E_Z$ , the energy conservation law will prevent a coupling of the (locally) incompressible quantum Hall states to nuclear spins. This result agrees with long nuclear spin relaxation times observed in experiments in the absence of charged excitations (at precisely  $\nu=1$  or  $\frac{1}{3}$  and at low temperature).

The situation changes dramatically when skyrmions are introduced into the 2DEG by either moving  $\nu$  away from 1 or  $\frac{1}{3}$ , increasing temperature, or applying voltage to induce electric current. The reason for the different behavior is the so-called “internal” spin excitations of skyrmions (in which their spin  $K$  changes by one) whose energy is much smaller than  $E_Z$  and can be brought into resonance with the nearly vanishing nuclear Zeeman energy. Moreover, we have checked that the oscillator strength  $\tau^{-1}$  of the skyrmion-nucleus collision corresponding to the  $K \leftrightarrow (K+1)$  transition is large and increases with increasing  $K$ .

In both IQH and FQH regimes, our results imply a critical dependence of the nuclear spin relaxation rate on the presence of skyrmions in the 2DEG, in good agreement with the experiments. The contrast between the forbidden relaxation due to spin waves and the efficient relaxation due to skyrmions should be more pronounced at  $\nu=1$  than at  $\nu=\frac{1}{3}$ , because of a larger (by an order of magnitude) interaction energy scale.

## ACKNOWLEDGMENTS

The authors acknowledge partial support by the Materials Research Program of Basic Energy Sciences, U.S. Department of Energy.

- 
- <sup>1</sup>K. von Klitzing, G. Dorda, and M. Pepper, *Phys. Rev. Lett.* **45**, 494 (1980).
- <sup>2</sup>R.B. Laughlin, *Phys. Rev. B* **23**, 5632 (1981).
- <sup>3</sup>D.C. Tsui, H.L. Störmer, and A.C. Gossard, *Phys. Rev. Lett.* **48**, 1559 (1982).
- <sup>4</sup>R.B. Laughlin, *Phys. Rev. Lett.* **50**, 1395 (1983).
- <sup>5</sup>F.D.M. Haldane, *Phys. Rev. Lett.* **51**, 605 (1983).
- <sup>6</sup>B.I. Halperin, *Phys. Rev. Lett.* **52**, 1583 (1984).
- <sup>7</sup>J.K. Jain, *Phys. Rev. Lett.* **63**, 199 (1989); A. Lopez and E. Fradkin, *Phys. Rev. B* **44**, 5246 (1991); B.I. Halperin, P.A. Lee, and N. Read, *ibid.* **47**, 7312 (1993).
- <sup>8</sup>*The Quantum Hall Effect*, edited by R.E. Prange and S.M. Girvin (Springer-Verlag, New York, 1987).
- <sup>9</sup>T. Chakraborty and P. Pietiläinen, *The Quantum Hall Effects* (Springer-Verlag, New York, 1995); *Perspectives in Quantum Hall Effects*, edited by S. Das Sarma and A. Pinczuk (Wiley, New York, 1997).
- <sup>10</sup>C.P. Slichter, *Principles of Magnetic Resonance* (Springer-Verlag, New York, 1990).
- <sup>11</sup>S.E. Barrett, R. Tycko, L.N. Pfeiffer, and K.W. West, *Phys. Rev. Lett.* **72**, 1368 (1994).
- <sup>12</sup>R. Tycko, S.E. Barrett, G. Dabbagh, L.N. Pfeiffer, and K.W. West, *Science* **268**, 1460 (1995); S.E. Barrett, G. Dabbagh, L.N. Pfeiffer, K.W. West, and R. Tycko, *Phys. Rev. Lett.* **74**, 5112 (1995).
- <sup>13</sup>N.N. Kuzma, P. Khandelwal, S.E. Barrett, L.N. Pfeiffer, and K.W. West, *Science* **281**, 686 (1998); P. Khandelwal, N.N. Kuzma, S.E. Barrett, L.N. Pfeiffer, and K.W. West, *Phys. Rev. Lett.* **81**, 673 (1998).
- <sup>14</sup>F.D.M. Haldane, in *The Quantum Hall Effect* (Ref. 8), Chap. 8, p. 303.
- <sup>15</sup>A. Wójs and J.J. Quinn, *Philos. Mag. B* **80**, 1405 (2000); J.J. Quinn and A. Wójs, *J. Phys.: Condens. Matter* **12**, R265 (2000); A. Wójs, *Phys. Rev. B* **63**, 125312 (2001).
- <sup>16</sup>T. Chakraborty, P. Pietiläinen, and F.C. Zhang, *Phys. Rev. Lett.* **57**, 130 (1986); E.H. Rezayi, *Phys. Rev. B* **36**, 5454 (1987); I. Szlufarska, A. Wójs, and J.J. Quinn, *ibid.* **64**, 165318 (2001).
- <sup>17</sup>R. Ramajaran, *Solitons and Instantons* (North-Holland, Amsterdam, 1982); D.H. Lee and C.L. Kane, *Phys. Rev. Lett.* **64**, 1313 (1990); E. Fradkin, *Field Theories of Condensed Matter Systems* (Addison-Wesley, Redwood City, CA, 1991).
- <sup>18</sup>S.L. Sondhi, A. Karlhede, S.A. Kivelson, and E.H. Rezayi, *Phys. Rev. B* **47**, 16 419 (1993); H.A. Fertig, L. Brey, R. Côté, and A.H. MacDonald, *ibid.* **50**, 11 018 (1994); A.H. MacDonald, H.A. Fertig, and L. Brey, *Phys. Rev. Lett.* **76**, 2153 (1996); X.C. Xie and S. He, *Phys. Rev. B* **53**, 1046 (1996); A.H. MacDonald and J.J. Palacios, *ibid.* **58**, R10 171 (1998).

- <sup>19</sup>H.A. Fertig, L. Brey, R. Côté, and A.H. MacDonald, Phys. Rev. Lett. **77**, 1572 (1996).
- <sup>20</sup>A. Wójs and J.J. Quinn, Solid State Commun. **122**, 407 (2002); Phys. Rev. B **66**, 045323 (2002).
- <sup>21</sup>L. Brey, H.A. Fertig, R. Côté, and A.H. MacDonald, Phys. Rev. Lett. **75**, 2562 (1995); C. Timm, S.M. Girvin, and H.A. Fertig, Phys. Rev. B **58**, 10 634 (1998); B. Paredes and J.J. Palacios, *ibid.* **60**, 15 570 (1999).
- <sup>22</sup>F.D.M. Haldane and E.H. Rezayi, Phys. Rev. Lett. **54**, 237 (1985).
- <sup>23</sup>C. Kallin and B.I. Halperin, Phys. Rev. B **30**, 5655 (1984).
- <sup>24</sup>A. Berg, M. Dobers, R.R. Gerhardts, and K. von Klitzing, Phys. Rev. Lett. **64**, 2563 (1990).
- <sup>25</sup>I.D. Vagner and T. Maniv, Phys. Rev. Lett. **61**, 1400 (1988); R. Côté, A.H. MacDonald, L. Brey, H.A. Fertig, S.M. Girvin, and H.T.C. Stoof, *ibid.* **78**, 4825 (1997); D. Mozysky, V. Privman, and I.D. Vagner, Phys. Rev. B **63**, 085313 (2001); T. Maniv, Y.A. Bychkov, I.D. Vagner, and P. Wyder, *ibid.* **64**, 193306 (2001).
- <sup>26</sup>J. Sinova, S.M. Girvin, T. Jungwirth, and K. Moon, Phys. Rev. B **61**, 2749 (2000).
- <sup>27</sup>K. Hashimoto, K. Muraki, T. Saku, and Y. Hirayama, Phys. Rev. Lett. **88**, 176601 (2002).
- <sup>28</sup>D. Loss and D.P. DiVincenzo, Phys. Rev. A **57**, 120 (1998); B.E. Kane, Nature (London) **393**, 133 (1998); G.P. Berman, G.D. Doolen, R. Mainieri, and V.I. Tsifrinovich, *Introduction to Quantum Computers* (World Scientific, Singapore, 1998).
- <sup>29</sup>H.D.M. Davies, R.L. Brockbank, J.F. Ryan, and A.J. Turberfield, Physica B **256-258**, 104 (1998); R.L. Brockbank, H.D.M. Davies, J.F. Ryan, M.A. Thomson, and A.J. Turberfield, Physica E (Amsterdam) **6**, 56 (2000).
- <sup>30</sup>S. Kronmüller, W. Dietsche, J. Weis, K. von Klitzing, W. Wegscheider, and M. Bichler, Phys. Rev. Lett. **81**, 2526 (1998).
- <sup>31</sup>A. Wójs and P. Hawrylak, Phys. Rev. B **51**, 10 880 (1995); J.J. Palacios, D. Yoshioka, and A.H. MacDonald, *ibid.* **54**, 2296 (1996).
- <sup>32</sup>T.T. Wu and C.N. Yang, Nucl. Phys. B **107**, 365 (1976); G. Fano, F. Ortolani, and E. Colombo, Phys. Rev. B **34**, 2670 (1986).
- <sup>33</sup>J.E. Avron, I.W. Herbst, and B. Simon, Ann. Phys. (N.Y.) **114**, 431 (1978); A. Wójs and J.J. Quinn, Physica E (Amsterdam) **3**, 181 (1998).
- <sup>34</sup>M.J. Snelling, G.P. Flinn, A.S. Plaut, R.T. Harley, A.C. Tropper, R. Eccleston, and C.C. Phillips, Phys. Rev. B **44**, 11 345 (1991); R.M. Hannak, M. Oestreich, A.P. Heberle, W.W. Ruhle, and K. Kohler, Solid State Commun. **93**, 3132 (1995).
- <sup>35</sup>A. Wójs, J.J. Quinn, and P. Hawrylak, Phys. Rev. B **62**, 4630 (2000); A. Wójs, P. Hawrylak, and J.J. Quinn, *ibid.* **60**, 11 661 (1999); A. Wójs, I. Szlufarska, K.-S. Yi, and J.J. Quinn, *ibid.* **60**, R11 273 (1999).
- <sup>36</sup>R.K. Kamilla, X.G. Wu, and J.K. Jain, Solid State Commun. **99**, 289 (1996).